Acta Mechanica Slovaca **27 (4): 22 - 35,** December **2023**
https://doi.org/10.21496/ams.2023.033

Acta Mechanica Slovaca
ISSN 1335-2393
www.actamechanica.sk

Enhancing Piping System Reliability Through Material Upgrades and ANN-Based Damage Parameter Estimation

Mohammed Amine Belyamna [1*], Abdelmoumene Guedri [1], Abdelhalim Aiiaoui [2], Chouaib Zeghida [1]

[1] Infra-Res Laboratory, Department of Mechanical Engineering, University of Souk Ahras, Algeria

[2] Department. of Mechanical Engineering, University of Khenchela, Algeria

Abstract: The objective of this study is to enhance the longevity of damaged or defective components through necessary repairs. In corrosive environments, stainless steels, such as 304 and 316NG austenitic stainless steel (SS), are preferred due to their chemical composition. Notably, 316SS contains a higher molybdenum content, resulting in improved resistance to pitting and crevice corrosion. The simulation of intergranular stress corrosion cracking (IGSCC) in SS piping relies on factors like applied and residual stresses, environmental conditions, and sensitization degree. To understand crack growth rates and times-to-initiation for each material, "damage parameters (DPs)" are utilized. These DPs consolidate the individual influences of various parameters. To estimate the DPs an artificial neuronal network (ANN) is proposed in this work. The ANN serves as a tool for predicting the DPs based on the given inputs. The obtained results are then utilized in numerical simulations to assess crack growth rates, times-to-initiation, and reliability for damaged 304SS and 316SS. Finally, this paper investigates the impact of replacing old 304 material with new 316NG material on piping reliability. By examining the effects of this replacement, the study aims to provide insights into how the reliability of the piping can be improved through material upgrades.

Keywords: ANN, damage, reliability, 304 and 316 austenitic piping, stress corrosion cracking.

1. Introduction

The field of nuclear materials science and structural reliability analysis has experienced significant progress and a growing body of research over the decades. A foundational document dating back to 1979 by the Nuclear Regulatory Commission (NRC) [1] investigates and evaluates stress corrosion cracking in the piping of Light Water Reactor (LWR) plants. This report highlights the early recognition of stress corrosion cracking as a critical concern for nuclear power systems. In 1987, Akashi and Ohtomo's work [2] evaluated the factor of improvement for the intergranular stress corrosion cracking life of sensitized stainless alloys in high-temperature, high-purity water environments. Their research provides valuable insights into the behavior of stainless alloys under specific conditions. A theoretical and user's manual for PC-Praise, a probabilistic fracture mechanics computer code developed by Harris and Dedhia in 1992, is presented in [3]. Endorsed by the US Nuclear Regulatory Commission (NRC), this code serves as a crucial tool for analyzing piping reliability. In 1994, Akashi [4] proposed an exponential distribution model for assessing the stress corrosion cracking lifetime of BWR component materials. This model offers a valuable framework for estimating the service life of materials under the influence of stress corrosion cracking. The work by Zhang et al. [5] delves into the

*** Corresponding author:** Mohammed Amine Belyamna, ***E-mail address:*** *m.belyamna@univ-soukahras.dz;*

initiation and propagation of IGSCC for sensitized type 304 stainless steel in dilute sulfate solutions. This study contributes to our understanding of the mechanisms behind IGSCC, a phenomenon of great concern in nuclear materials. Ting's work [6] evaluates IGSCC problems in stainless steel piping at the Taiwan BWR-6 nuclear power plant, shedding light on localized issues within specific nuclear installations.

Further advancements in reliability analysis and prediction are presented in [7] to [10], which explore techniques such as neural networks and Monte Carlo simulations (MCS) for assessing structural integrity and reliability under various conditions. Meireles et al. [11] provide a comprehensive review of the industrial applicability of artificial neural networks, emphasizing their role in modern reliability engineering. Additionally, [12] documents proceedings from a seminar on Materials Research and Development for Prototype Fast Breeder Reactors (PFBR), emphasizing the importance of materials research in advanced reactor systems. Jones [13] focuses on mitigating corrosion problems in LWRs through changes in water chemistry, underlining the significance of chemistry alterations in combating corrosion issues. The International Atomic Energy Agency (IAEA) plays a crucial role in setting standards for the assessment and management of aging major nuclear power plant components. [14] provides guidelines for ensuring the safety and reliability of BWR pressure vessels.

[15] to [33] represent a wide range of recent research efforts encompassing topics such as artificial neural networks, corrosion defects in pipelines, failure analysis of corroded high-strength pipelines, and reliability prediction using MCS.

Due to their suitable high-temperature properties, which include high creep strength, resistance to low cycle fatigue and creep-fatigue interactions, and good resistance to environmentally sensitive cracking, austenitic stainless steels are preferred as the primary structural materials in a variety of industries. Their selection is supported by the availability of code data on mechanical parameters and their better weldability [12].

Making sure that the items they produce meet or exceed quality and performance standards requires a lot of work and commitment on the part of manufacturers. However, the effect on the bottom line can be enormous if faulty products are not performing properly. Calculating the product's reliability and longevity is crucial. When that product comes back damaged, you either need to repair it as a replacement. When corrosion resistance is desired, ferrous metals such as 304SS and 316SS are frequently utilized. They continue to offer durable solutions in many industries and are a superb answer in challenging conditions. Let's explore stainless steel in more detail and attempt to determine what renders 304SS and 316SS different. The impact of repairing or replacing 304SS material with a higher grade 316SS following a necessary repair will be examined in the sections that follow. Both materials' models were created.

For each material, the crack growth rates and times-to-initiation are compared against "DPs," which combine the various contributions of various individual parameters. The DPs used in this work are multiplicative relationships between various terms that each describe how different phenomena, such as the environment (specifically coolant temperature, dissolved oxygen content, and levels of impurities), applied loads (including both constant and variable loads to account for steady-state operation and, respectively, plant loading or unloading), residual stresses, and material sensitization) affect SCC behavior [5], [24], [27]. To accomplish this, a two-step approach is suggested.

1. ANN for DPs Estimation: In the first step, an ANN is proposed to estimate the DPs based on the various independent inputs. The ANN is trained using a dataset that includes the independent inputs and corresponding DPs. By learning from this dataset, the ANN can establish a relationship between the inputs and the DPs, allowing it to estimate the DPs for new sets of independent inputs. This estimation provides crucial input for the subsequent steps in the analysis.

2. Numerical Simulation for Crack Growth Rates, Times-to-Initiation, and Reliability Assessment: In the second step, the estimated DPs obtained from the ANN are utilized in a mathematical simulation to determine crack growth rates, times-to-initiation, and the reliability of damaged material. The simulation takes into account various factors such as material properties, loading conditions, and environmental effects to model the crack growth behavior accurately.

The reliability model, which was developed in previous work [33], is adapted specifically for evaluating the probability of failure in 316SS piping. This model incorporates the estimated DPs and utilizes probabilistic methods to assess the reliability of the piping system. By considering the uncertainties and variability associated with the inputs and DPs, the reliability model provides

insights into the likelihood of failure under given conditions. By employing this two-step approach, combining the ANN-based estimation of DPs with mathematical simulations and reliability analysis, it becomes possible to comprehensively evaluate the behavior of damaged 316SS piping and assess its probability of failure. This methodology enhances understanding and decision-making regarding maintenance, repair, or replacement strategies for such piping systems.

2. Damage prediction

2.1 Experimental data sets

The investigation of the susceptibility of 304SS and 316SS to stress corrosion cracking (SCC) under nuclear power plant operating conditions is of utmost importance for ensuring the safety and integrity of components manufactured from these materials. The experimental methodology expounded in [3] is considered critical for this purpose. In this regard, representative samples of 304SS and 316SS, specifically designed for nuclear applications due to their enhanced resistance to corrosion, were selected by the laboratory staff. To simulate the service conditions in nuclear power plants, specimens were prepared with standardized geometries, such as tensile bars of 50.4mm, and specific environmental conditions were identified. In some instances, high-temperature water with specific chemical additives or the simulation of primary and secondary water chemistry may be used in SCC initiation tests.

A regular inspection of the specimens was conducted to detect the presence of cracks, including microcracks and corrosion pits. The time taken for SCC cracks to initiate under the applied stress and environmental conditions was recorded. This information is vital for comprehending SCC initiation kinetics and determining the critical stress intensity factors associated with SCC initiation.

In [3], the variation of key parameters, such as stress levels, temperature, and environmental conditions, was used to assess their impact on SCC initiation. Statistical methods and mathematical models were utilized to quantify the initiation behavior under different conditions.

The time to crack initiation under static load conditions was discovered to be a function of the DP, as presented in Eq. (1). Hence, the time to crack initiation tI for a given DP was assumed to be log-normally distributed. The mean and standard deviation of Log (tI) are provided in [3].

Mean value of $\text{Log}(t_I)=C_{10}\text{-}C_{11}\text{aLog}(D\sigma)$ and Standard deviation of $\text{Log}(t_I=)C_{11}$ (1)

The damage parameter DP represents the effects of loading, environment, and material variables on IGSCC and is given by

$\text{DPs}=f_1(\text{material})xf_2(\text{enviroment})xF_3(\text{looding})$ (2)

where f_1, f_2 and f_3 are given by

$$f_1 = C_1(Pa)^{C_2} \quad (3)$$

$$f_2 = O_2^{C_3}\exp\left[C_4/(T+273)\right]\log(C_5\gamma^{C_6}) \quad (4)$$

$$f_3 = (C_8\sigma^{C_9})^{C_7} \quad (5)$$

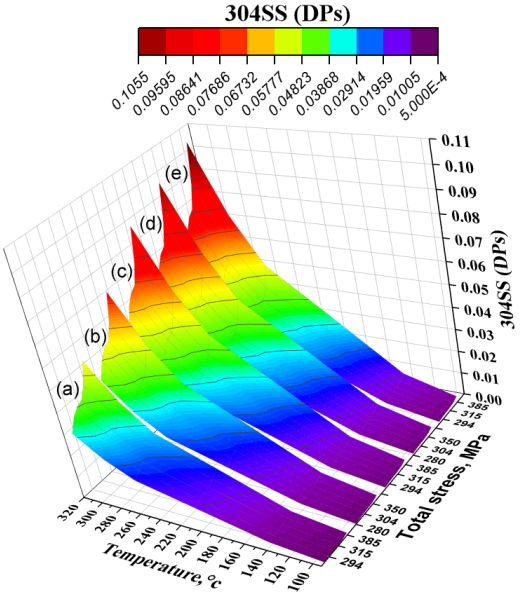

Figure 1a: displays the 304SS DPs at different temperatures and varying levels of applied stress. The conductivity is fixed at 0.51 µS/cm, and the measurements are taken under steady-state conditions for different O_2 content levels: 0.2ppm (Case a), 1ppm (Case b), 2ppm (Case c), 8ppm (Case d), and 16ppm (Case e).

Where Pa is a measure of degree of sensitization, given by Electrochemical Potentiokinetic Reactivation in C/cm^2, O_2 is oxygen concentration in ppm, T is temperature in degrees centigrade, γ is water conductivity in µs/cm, and σ is stress in MPa. In the above equations, C_I are constants whose values depend on the type of material.

The current study was conducted in two locations, namely [3] and [21]. The presented dataset is focused on the examination of welds in 304/316

SS piping following 50 years of plant operation and is demonstrated in Figures 1(a and b). The DPs are represented as numerical values that consolidate the individual influences of various parameters on crack growth rates and times-to-initiation for each material. Figure 1a depicts a graphical representation of the DPs for 304SS at different temperatures and levels of applied stress. The conductivity of the material remains constant at 0.51µS/cm, which is an indicator of its electrical conductivity. The measurements were obtained under steady-state conditions, signifying that the system was in a stable and unchanging state. Different levels of O_2 content are represented by different cases, including 0.2ppm (Case a), 1ppm (Case b), 2ppm (Case c), 8ppm (Case d), and 16ppm (Case e).

Similarly, in Figure 1b, the DPs are influenced by varying levels of oxygen (O_2), applied stress, and a constant conductivity of 0.51 µS/cm. The measurements were obtained under steady-state conditions at different temperatures, including 93°C (Case a), 140°C (Case b), 204°C (Case c), 260°C (Case d), and 288°C (Case e).

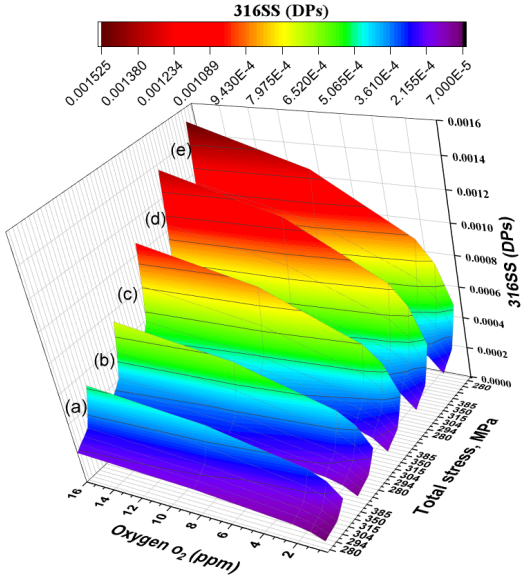

Figure 1b: illustrates the DPs of 316SS concerning varying levels of O_2, applied stress, and a constant conductivity of 0.51 µS/cm. The measurements were taken under steady-state conditions, with the following temperature settings: T= 93°C (Case a), T= 140°C (Case b), T= 204°C (Case c), T= 260°C (Case d), and T= 288°C (Case e).

Table 1a: Statistics of input variables

	Stress [MPa]	*Pa [C/cm2]*	*02 [ppm]*	*T [°C]*
Mean	325,42	31,01	5,44	216,66
Standard Deviation	33,67	35,25	5,95	79,57
Standard error of the mean	0,83	0,87	0,14	1,97
Upper limit of the 95% confidence interval of the mean	327,06	32,73	5,73	220,54
Lower limit of the 95% confidence interval of the mean	323,78	29,29	5,14	212,78
Number of observations	1620	1620	1620	1620

Table 1a exhibits a set of four input variables, namely Stress, Pa, O_2, and T, accompanied by their corresponding statistical measures. Stress is gauged in MPa, Pa is measured in C/cm^2 (Coulomb per square centimeter), O_2 is measured in ppm (parts per million), and T is measured in degrees Celsius. The statistical measures presented in the table include Mean, Standard Deviation, Standard error of the mean, Upper limit of the 95% confidence interval of the mean, Lower limit of the 95% confidence interval of the mean, and Number of observations.

Table 1b: Statistics of output variables

	304SS (DPs)	*316SS (DPs)*
Mean	$2{,}57\times10^{-2}$	$4{,}79\times10^{-4}$
Standard deviation	$2{,}79\times10^{-2}$	$2{,}99\times10^{-4}$
Standard error of the mean	$6{,}93\times10^{-4}$	$7{,}44\times10^{-6}$
Upper limit of the 95% confidence interval of the mean	$2{,}71\times10^{-2}$	$4{,}93\times10^{-4}$
Lower limit of the 95% confidence interval of the mean	$2{,}44\times10^{-2}$	$4{,}64\times10^{-4}$
Number of observations	1620	1620

Table 1b provides statistical information about two output variables, namely "304SS (DPs)" and "316SS (DPs)". The statistical metrics employed are identical to those explicated in Table 1a.

2.2 Artificial Neural Network Model

This study introduces the basic concepts of ANNs, a powerful tool for solving complex problems that cannot be easily expressed with a formula. ANNs are often compared to the human brain due to their architecture and abilities. ANNs consist of a network of simple processing units

(nodes) whose processing capacity is stored in the interunit connection strengths (weights) obtained through training on a set of patterns. Different learning algorithms can be used depending on the training data and expected output. ANNs can learn from samples and implicitly detect complicated nonlinear interactions between variables. The ANN is commonly used for supervised learning which consists of three layers (I, H, and O), with I denoting the number of nodes in the input layer, H denoting the number of nodes in the hidden layer, and O denoting the number of nodes in the output layer. These three layers are highly interconnected by nodes and work together to solve specific problems.

Once the data is received in the input layer the processed values are sent to the hidden layer. The hidden layer and output layer process all incoming signals by applying some weights to them. The ANN uses an algorithm for training networks where the error at the output layer is moved back to the input-hidden layers for updating weights and decreasing errors to yield the best results. The primary objective of the ANN process is to decrease the total error between the observed and predicted values by adjusting the weights. These weights are combined and processed through an activation function and released to the output layer [7-8].

In looking for the best ANN model, one has to determine the appropriate number of hidden layers and the number of neurons in each one. This is done through training and testing of different network structures and the aone should ultimately be determined by evaluating tolerance between predicted and experimental data. Mean square error, MSE, indicator as shown in Eq. (6) was introduced to evaluate the training and generalization

$$MSE = \frac{1}{N}\sum_{i=1}^{N}(t_i - y_i)^2 \qquad (6)$$

performances of ANN [11] and [14].

where ti and yi are experimental and predicted DP values, respectively, and N is the number of data sets.

The ANN used in this study has forth input parameters (I=4), two hidden layers with ten hidden layer nodes (H=10), and two output layer nodes (O=DPs). The hyperbolic tangent transfer function and the linear transfer function are utilized as activation functions in the hidden and output layers, respectively. The Levenberg-Marquardt (LM) algorithm is used to train the network. Figure 2 shows the resulting neural network's architecture.

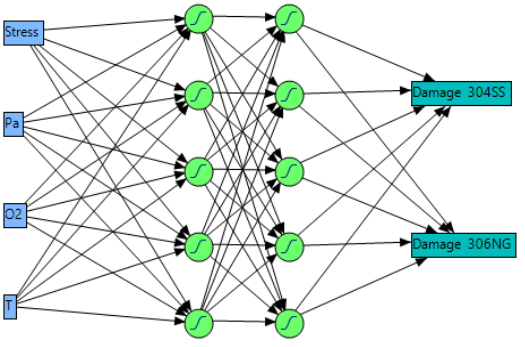

Figure 2: The architecture of the optimal ANN model to predict DPS

3. Evaluation of Piping Reliability

This section presents the methodology recommended by [3, 21, 22, 23, 24] for modeling IGSCC in stainless steel pipes, which is based on two-dimensional semi-elliptical interior surface cracks that are typically circumferentially oriented. The overall time to pipe leaks is separated into three steps: time to initiate a very small crack, time spent growing small cracks at an initiation velocity, and time spent growing larger cracks at fracture mechanics velocity to become through-wall cracks. The DPs, which are a function of material, environment, and loading variables, are used to determine the time to crack initiation. This study considers both breakage and leakage as potential failure modes, with part-through initial stress corrosion cracks potentially growing into unstable part-through or through-wall cracks.

The failure criterion for pipe leakage is defined as a = h, where h is the wall thickness and a is the crack depth, and the stability of the crack is determined by comparing net-section stress with the flow stress of the material. The net-section stress criterion applies to very tough material, and the failure is due to insufficient remaining area to support the applied loads given by Eqs. (7) and (8), i.e., net-section stress due to applied loads becomes greater than the flow stress of the material.

$$\sigma_{net} = \frac{\sigma_{LC} A_p}{A_p - A_{cr}} \rangle \sigma_f \qquad (7)$$

$$A_p = \pi h(2R_i + h)$$

$$A_{cr} = ab\left[2 + \left(\frac{a}{R_i}\right)\right] \qquad (8)$$

where Ri is the internal radius of pipe, h is the pipe wall thickness, A_p is the cross-section area of the pipe, is the area of crack, σ_{LC} and σ_f are the load-controlled components of stress and the flow stress, respectively.

To predict the reliability of corroded pipes, ANNs with limited input parameters are used to ensure calculation efficiency and avoid overlearning. However, arbitrarily reducing parameters can affect the accuracy of the ANN's prediction [28]. A sensitivity analysis is performed to determine the primary parameters to retain in the ANN model. Due to the low probability of pipe failure, appropriate statistical methods, such as the Monte Carlo Simulation (MCS), are used to obtain sufficient data for reliability analysis. The entire MCS database is divided into three groups for ANN training, testing, and validation (see Figure 3).

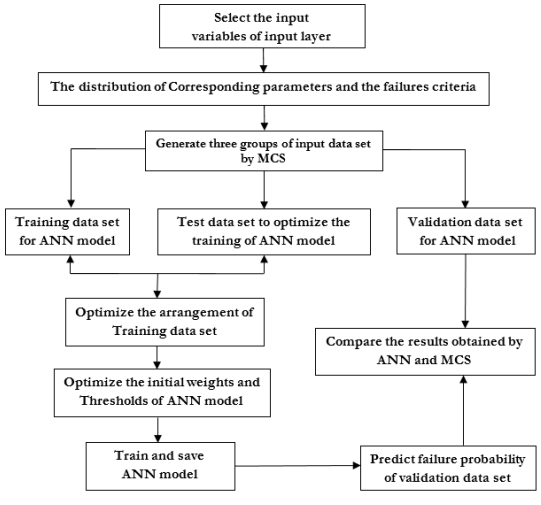

Figure 3: Presents a flow chart outlining the methodology proposed for this study

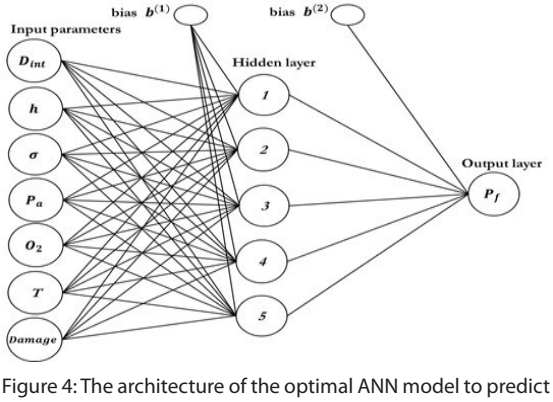

Figure 4: The architecture of the optimal ANN model to predict the probability of failure

The best ANN model is determined by evaluating tolerance between predicted and actual data, with the input variables including DP values, applied stress levels, steady-state temperatures, O_2 content, and periods of plant operation. The output variable is the failure probability. The Levenberg-Marquardt algorithm is used to train the ANN, resulting in a network of one hidden layer with five neurons (See Figure 4).

4. Results and Discussions

4.1 Damage prediction

Figures. (5a, b - 6a, b) shows the correlation between the observed and predicted DPs of both materials versus the service operating conditions for both training and testing for the selected model.

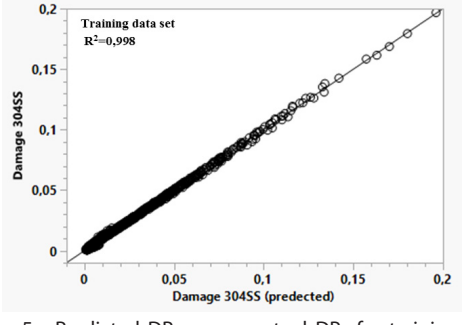

Figure 5a: Predicted DPs versus actual DPs for training data (304SS)

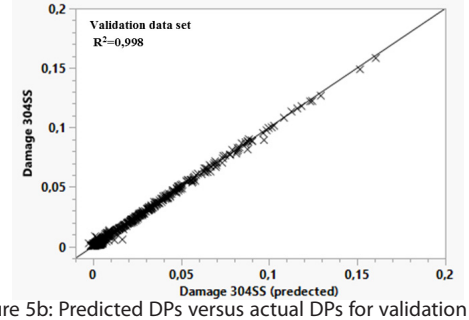

Figure 5b: Predicted DPs versus actual DPs for validation data (304SS)

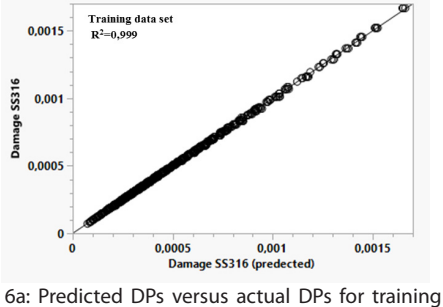

Figure 6a: Predicted DPs versus actual DPs for training data (316SS)

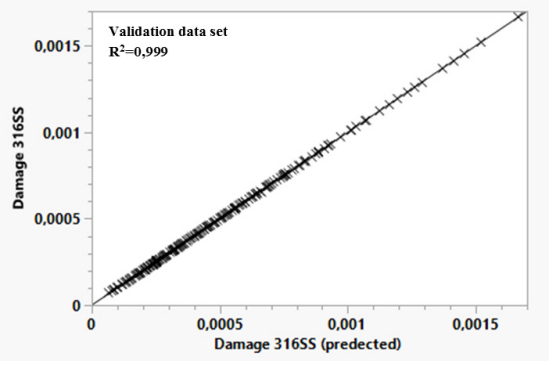

Figure 6b: Predicted DPs versus actual DPs for validation data (316SS)

The significance is a measure of how much the inputs influence the output. Each variable was investigated for the best model and presented in Figure 7. However, each input was seen to offer at least a moderate contribution to the output. This, therefore, confirmed that they were a good choice of inputs. In summary, it was important to find out which variables are considered to be most significant, or those that contributed very little to the output. However, it is well understood that many of the variables have some bearing on steel strength. Overall, the aim was to obtain meaningful inputs that allow the optimization of mechanical properties within a predictive framework.

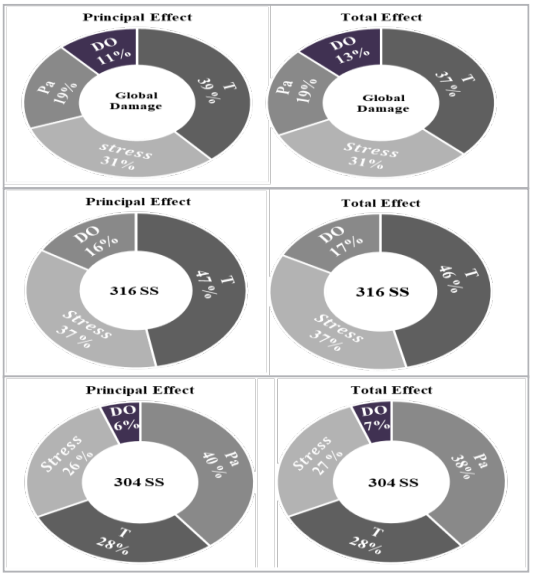

Figure 7: Showing a measure of the model's perceived significance of each input variable influencing the outputs as deduced from the network

Once the model was developed, its behavior was compared to findings in the literature. The aim was to show that it agrees with existing data and has enough complexity to describe different relationships. To validate this, a random 5% of the same database are used to estimate the damage levels using a nonlinear multiple regression model developed in [3] given by Eqs. 2 to 5 for both materials.

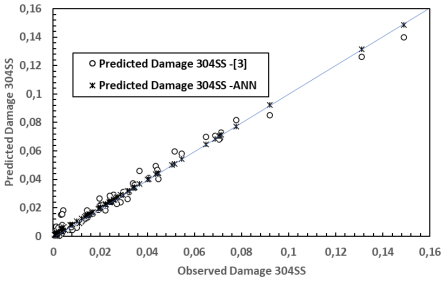

Figure 8: Comparison of the predicted function of observed DP values for 304SS using nonlinear regression [3] and ANN

Figures. (8-9) show that the ANN (R2= 0.999) performs better at evaluating the DPs than the nonlinear regression model; (R2= 0.929) created in [3].

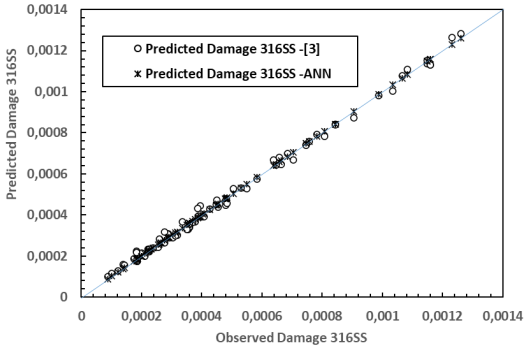

Figure 9: Comparison of the predicted function of observed DP values for 316SS using nonlinear regression [3] and ANN

It would be interesting to find any nonlinear relationships that are not captured by linear regression methods. This would show that the flexibility of ANN may be more suitable for making predictions. To illustrate this, 3D plot examples of DPs were made for total stress, temperature, and dissolved oxygen (Figures.10a, b-11a, b).

The brown, green and blue color ranges shown in figures (10a, b-11a, b) respectively indicate the ranges of damage variation, which can be classified into three categories: high, medium and low.

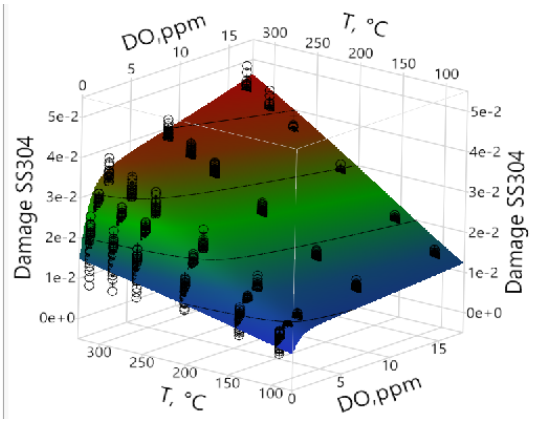

Figure 10a: Predicted DPs of 304SS material versus DO and temperature (Pa=10 C/cm² and Stress=350 MPa)

In Figure 10a, a graph is presented that shows the predicted damage parameters (DPs) of 304 SS material. The graph plots the DPs against two variables, dissolved oxygen, and temperature, under specific conditions, including a stress of 350 MPa and a pitting corrosion potential of 10 C/cm². The graph shows that under low DO values of less than 0.2 ppm, an increase in temperature results in low damage, while high DO values and high temperatures result in high damage.

Figure 10b also presents a graph that shows the predicted DPs of 304 SS material with DPs plotted against pressure and temperature. The stress applied to the material is 300 MPa, and the dissolved oxygen concentration is 0.2ppm. As per Figure 7, 304 SS material is sensitive to Pa, and Figure 10b confirms that low Pa values of less than 20 C/cm² result in low damage.

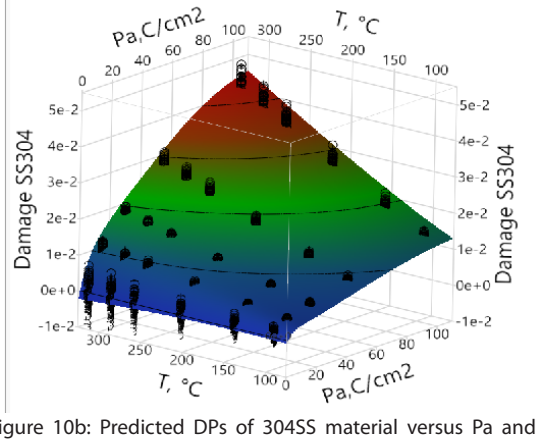

Figure 10b: Predicted DPs of 304SS material versus Pa and temperature (Stress=300 MPa and DO=0.2 ppm)

Moving on to Figure 11a, it displays the predicted DPs of 316SS material, illustrating how the DPs vary as the stress and temperature change. The prediction is based on specific conditions, including a Pa of 8 C/cm² and a dissolved oxygen concentration of 0.2 ppm. It shows that low damage is always a result of a combination of minimum load and temperature.

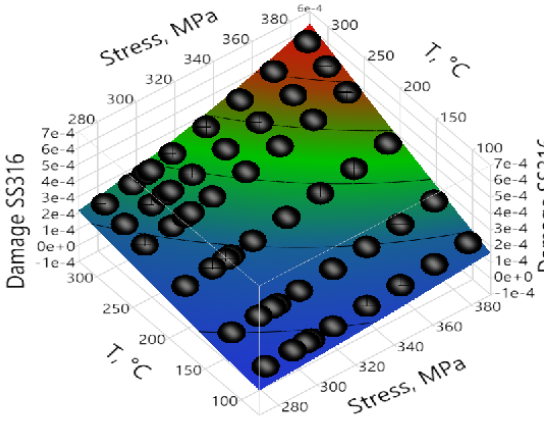

Figure 11a: Predicted DPs of 316SS material versus total stress and temperature (Pa=8 C/cm² and DO=0.2 ppm)

Finally, Figure 11b portrays the predicted DPs of 316 SS material, plotting the DPs against two variables: total stress and dissolved oxygen. The DPs are measured at Pa of 8 C/cm², and the temperature is set at 325 °C. The graph shows that the 5E-4 iso-value line delimits weak damage.

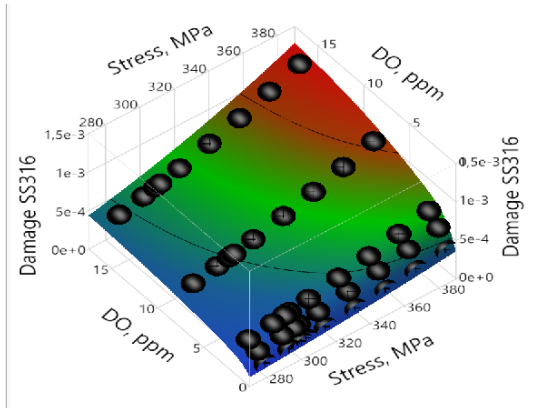

Figure 11b: Predicted DPs of 316SS material versus total stress and DO (Pa=8 C/cm² and T=325°C)

4.2 Reliability Evaluation

This section aims to investigate the impact of modifying environmental parameters, such as oxygen concentration and temperature during operation, as well as the replacement of 304SS material with higher-grade 316SS material after

repair. While the model was initially developed for 304SS, adapting it for 316SS was a straightforward process of defining new damage parameters using relevant laboratory data. The underlying structure of the model remained the same. The theoretical model, developed by comprehending the cracking mechanism, effectively predicts observed damage accumulation [2], as depicted in Figure 12.

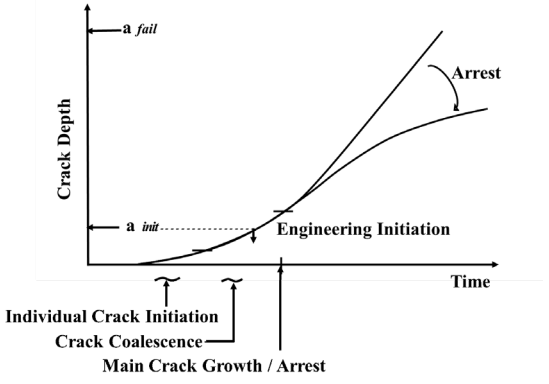

Figure 12: Effect of crack initiation, coalescence, and growth during subcritical cracking in aqueous media [2]

The reliability model used in this investigation is tested using original data from [2]. The results are shown in Figure 13. The resulting predictions had a much more rational basis and were in very good agreement with operational data for periods beyond 6 years. The less satisfactory level of agreement for periods less than 6 years can be attributed in a large measure to the lack of observed failure events for the early periods of plant operation.

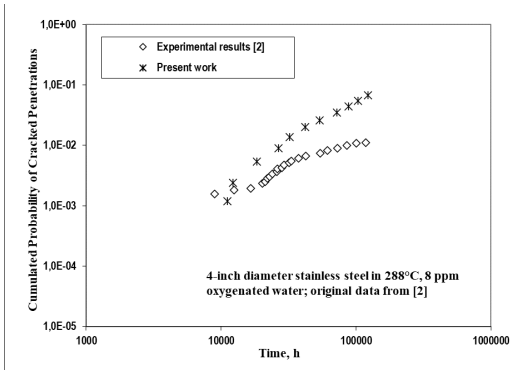

Figure 13: Probability as a function of time of stress corrosion crack initiation in 4-inch diameter sensitized stainless steel in 288 ° C, 8 ppm hydrogen peroxide; original data from [2]

In this part our main objective is to study the relative behavior of different types of materials under otherwise nominally identical conditions presented in Table 2:

A service life of 50 years is simulated and the results are printed every two years. The maximum time step for stress corrosion crack growth is limited to 0.1 years, which means that even during a long period of steady-state operation, the crack size, stress intensity factors, and other calculations are updated every 0.1 years. In the output file, there is a description of the data. In addition to the initiation probability, the leakage probabilities as a function of time and the rupture probability are obtained in the same run.

4.2.1 Comparative Study of the Effect of Changing the O_2 Concentration After Repair

Table 3 shows the damage for a given temperature of 288°C as a function of the concentration of O_2 in the range of 0.05 to 8 ppm, corresponding to the cases studied.

Table 3: Damage as a function of DO

DO [ppm]	0.05	0.2	2	8
Damage 304SS	1.24E-3	1.59E-3	1.27E-3	3.09E-3
Damage 316SS	2.83E-4	3.94E-4	6.85E-4	9.55E-4

Figures 14 to 15 provide an example of information on the number of cracks that are initiated at the start of the time increment during that trial, and the number of cracks that are initiated within the time increment (Total initiated cracks by initiation and coalescence). Such results are printed out for each evaluation time. Note that initiation in a 304SS weld reaches its maximum after only about 4 years of operation, while in the 316SS type, this threshold is crossed only after 12 years. The reason for this difference is clear from Figures 14 to 15, which show the initial and total number of crack initiations in 304SS and 316SS materials. Note also that cracks begin to initiate in 304SS during the first year of operation; by the time the first initiation occurs in 316SS (about four years), nearly 4640 cracks have initiated in the lower strength material.

The ratio of 316SS initiated cracks to 304SS initiated cracks for a temperature of 288°C and an O_2 level of 0.05 ppm drops to less than 287 at two years and less than 3 at ten years and less than one at the end of the plant's life (see Figure 16). In any case, 316SS has good corrosion resistance mainly because fewer initiated cracks than in 304SS, and those that are initiated generally contribute later in the life span. However, once a crack has been initiated, its subsequent growth rate is not significantly affected by material type.

Table 2: Input values for parametric calculation

	304SS	*316SS*
Pipe geometry [mm]	Inner radius = 364 Wall Thickness = 21.3	
Pipe loading values [MPa]	Stress due to OP = 35.21 Total applied stress = 176.61	
Material flow stress [MPa]	Normally Distribute: Mean value = 314.3 Standard deviation = 13.3	
SCC Parameters	O2 at startup [ppm] = 8.00 O2 at steady state [ppm] = as per Tabe 3 Temp. at steady state [°C] = as per Tabe 4 Heat up (38-288[°C]) Time [HRS] = 5.00 Coolant conductivity [µS/cm] = 0.20	
Initial flow distribution [mm]	Lognormal distribution Deterministic flaw depth = 0.025 Mean flaw length =3.2 Shape parameter =0.85	

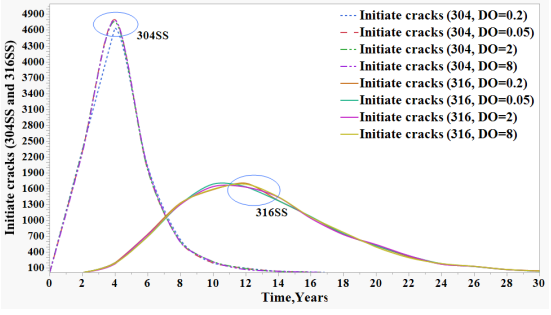

Figure 14: Number of cracks initially initiated in the two types of materials for a temperature of 288°C and different DO values

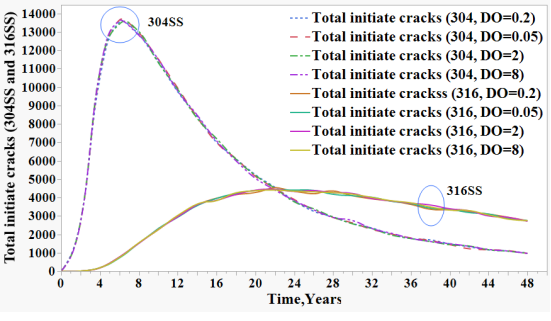

Figure 15: Number of cracks total initiated in the two types of materials for a temperature of 288°C and different DO values

Figure 17 shows, the cumulative leakage probabilities of the four cases treated. The results are given for both the original 304SS material and the replacement 316SS material. In 304SS piping, a leak should occur after two years of operation (i.e., the

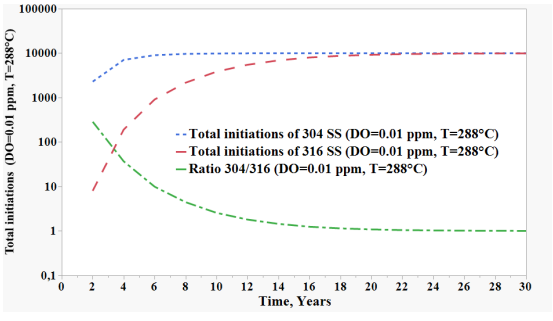

Figure 16: Total initiations of both 304SS and 316SS materials for a temperature of 288 °C and oxygen reduction to 0.01 ppm. (Monte-Carlo simulation of 10000 replications)

cumulative probability of leakage approaches this). While it is important to keep in mind the conservatism of the analysis, this result is nevertheless reasonably consistent with some field observations [2, 4]. Assuming the original piping configuration remains unchanged, replacing 304SS with 316SS results in virtually no leakage probabilities up to 6 years (with DO, at 0.2 ppm) and up to 12 years (with DO, at 0.05 ppm) of operation.

The leakage probability of 316SS first exceeds 10-4 after about 6 years, increasing to about (1,38E-01 for DO=0.05 ppm to 2,97E-01 for DO=0.2 ppm) at 30 years of the service life.

In the case of replacement by 316SS, the probability of leakage at the 30-year drops by about a factor (4.27 for a DO level of 0.2 ppm, 5.4

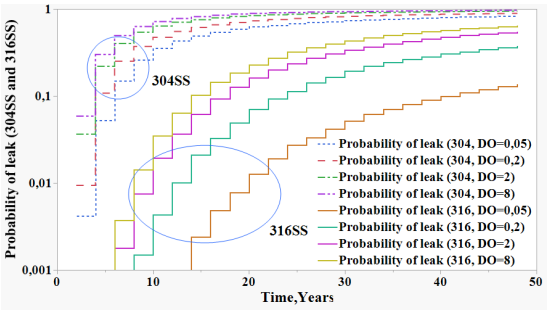

Figure 17: Cumulative leakage probabilities of the two types of materials for a temperature T=550 and different DO values

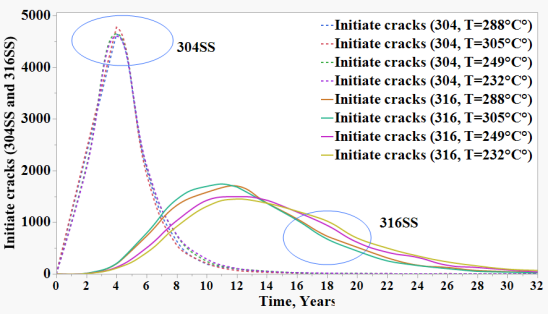

Figure 18: Number of cracks initially initiated in the two types of materials for a DO= 0.2 ppm and different temperature

for a DO level of 0.05ppm, 6.26 for an oxygen level of 0.01ppm).Failure of 304SS piping is always dominated by initiated cracks (i.e., resulting from stress corrosion), in 316SS, initiated cracks dominate the probability of leakage only after about 6 years. Once cracks are present, the growth rates are nominally the same in both materials. Therefore, the expected difference in behavior between the two materials is due to differences in the number of initiated cracks and their subsequent initiation time, rather than how these cracks would grow once initiated.

4.2.2 Comparative Study of the Effect of Changing the Temperature After Repair

Table 4 shows the damage for a given concentration of DO of 0.2 ppm as a function of temperature in the range of 232 to 305°C, corresponding to the cases studied.

For low damage (Table 4) the temperature variation does not influence the initiation process. Notice that initiation in a 304SS weld reaches its maximum after only about 4 years of operation, while in 316SS, this threshold is not crossed until after 12 years, this difference is justified from Figures. 18 to 19, which shows the initial and total number of crack initiations in 304SS and 316SS materials.

Table 4: Damage as a function of temperature

Temperature [°C]	232	249	288	305
Damage 304SS	1.13E-3	1.42E-3	1.59E-3	1.61E-3
Damage 316SS	3.26E-4	3.47E-4	3.94E-4	4.01E-4

Note also that cracks begin to initiate in 304SS during the first year of operation; by the time the first initiation occurs in 316SS (about four years),

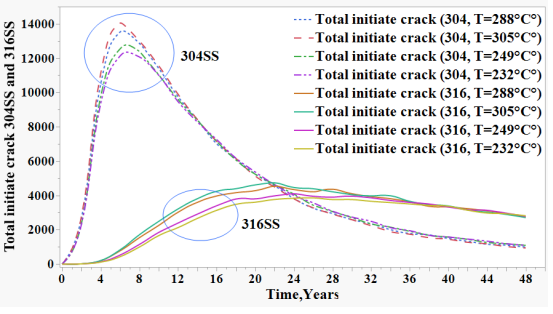

Figure 19: Number of cracks total initiated in the two types of materials for a DO= 0.2 ppm and different temperature

nearly 4640 cracks have initiated in the lower strength material. The ratio of 316SS initiated cracks to 304SS initiated cracks for DO of 0.2 ppm and at the lower temperature of 232°C drops to less than 340 at two years, less than 57 at four years, less than 4 at ten years, and less than one (1) at the end of the structure's life (see Figure 20). For DO of 0.2 ppm and a temperature decrease to 249°C drops to less than 69 at four years and less than 5 at ten years and less than one (1) at the end of the structure's life.

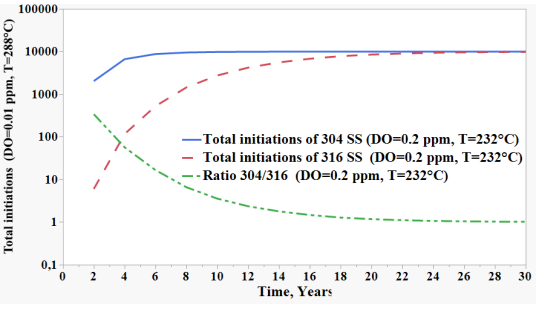

Figure 20: Total initiations of both 304SS and 316SS materials for a DO= 0.2 ppm and temperature reduction to 232 °C. (Monte-Carlo simulation of 10000 replications)

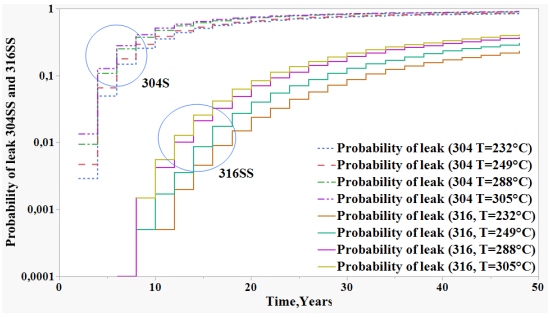

Figure 21: Cumulative leakage probabilities of the two types of materials for a DO= 0.2 ppm and different temperature

Figure 21 shows, the cumulative leakage probabilities of the four cases treated. The results are given for both the original 304SS material and the replacement 316SS material. In the 304SS piping, leakage is expected to occur after two years of operation. If 304SS is replaced by 316SS while maintaining the original piping configuration the corresponding leakage probabilities are nominally zero before 6 years of operation. The leakage probability first exceeds 10-4 after about 4 years and increases to about (5.00E-04 for T=232°C to 4,30E-03 for T=288°C) at 10 years of the service life. In the case of replacement by 316SS, the probability of leakage at the 30-year drops by about a factor (8.69 for T=232°C, 4.27 for T=288°C).

5. Conclusion

In this study, ANN soft computing tool is used to predict the SCC damage level of welded piping. Out of 1620 experimental data sets, 2/3 of the data sets are used for training and testing the network models and 1/3 of the data sets are used to validate the network models. An ANN model for fourth input nodes and two output nodes with two hidden layers starting from the tenth node was constructed and analyzed by using the LM algorithm. For the architecture of 4-5-5-2, the ANN model gave an optimum result. Further with the increase in the number of hidden layer nodes, the output remains the same or slightly improves, this could be owing to overfitting the output values. Here we obtained higher CC and lower MSE values by using only 5 nodes in 2 hidden layers. The proposed method is illustrated by several examples of 304SS and 316SS pipes subject to SCC. This optimal ANN can be used to effectively and accurately estimate the damage and the reliability of damaged pipes in the same service conditions.

The analysis of results from the treated cases reveals how changes in environmental parameters significantly impact the probability of a leak. The figures mainly display statistics related to cracks that were initiated over time. While many cracks were predicted to start forming, none managed to develop into through-thickness cracks during the entire 50-year simulated life of the pipe. Regarding low-damage situations, we observed that variations in temperature and oxygen concentration do not affect the crack initiation process. However, reducing these factors does contribute positively to lowering the probability of a leak occurring. In aggressive environments, it is advisable to use grade 316SS or higher-quality materials for optimal performance and longevity. Additionally, for damaged materials, we recommend replacement under specific, well-defined conditions that are deemed favorable for effective replacement.

Acknowledgments: The authors acknowledge the Ministry of Higher Education and Scientific Research, Algeria, for technical and financial support (Project code. A01L09UN410120200002).

References

[1.] Nuclear Regulatory Commission, Washington, DC (USA) (1979). Investigation and evaluation of stress-corrosion cracking in piping of light water reactor plants (NUREG--0531). United States.

[2.] Akashi, M., Ohtomo, A. (1987). Evaluation of the Factor of Improvement for the Intergranular Stress Corrosion Cracking Life of Sensitized Stainless Alloys in High-Temperature, High-Purity Water Environment. Journal of the Society of Materials Science, Japan, 36(400), pp.59–64.

[3.] Harris, DO., Dedhia, DD. (1992). Theoretical and user's manual for PC-PRAISE. A probabilistic fracture mechanics computer code for piping reliability analysis, US Nuclear Regulatory Commission, Washington, DC. July, NUREG/CR-5864, UCRL-ID-109798.

[4.] Akashi, M. (1994). An Exponential Distribution Model for Assessing the Stress Corrosion Cracking Lifetime of BWR Component Materials, Proceedings of Symposium on Life Prediction of Corrodible Structures, Ed. R.N. Parkins, Pub. NACE, 2, pp.1040-1049.

[5.] Zhang, S., Shibata, T., Haruna, T. (1997). Initiation and propagation of IGSCC for sensitized type 304 stainless steel in dilute sulfate solutions, Corrosion Science, Vol. 39, n.9, pp.1725-1739. Doi: 10.1016/S0010-938X(97)00078-4.

[6.] Ting, K. (1999). Evaluation of intergranular stress corrosion cracking problems of stainless steel piping in Taiwan BWR-6 nuclear power plant, Nuclear Engineering and Design,

191(2), pp. 245–54. Doi: 10.1016/S0029-5493(99)00146-6.

[7.] Ehrnsten, U., Aaltonen, P.A., Nenonen, P., Hanninen, H.E., Jansson, C., Angeliu, T.M. (2001). Intergranular cracking of AISI 316NG stainless steel in BWR environment, Environmental Degradation of Materials in Nuclear Power Systems — Water Reactors (Proc. 10th Int. Conf. Lake Tahoe NV, 2001) NACE (2001).

[8.] Papadrakakis, M., Lagaros, N.D. (2002). Reliability-based structural optimization using neural networks and Monte Carlo simulation, Computer Methods in Applied Mechanics and Engineering, 191(32), pp. 3491–507. Doi: 10.1016/S0045-7825(02)00287-6

[9.] You, J.S., Wu, W.F. (2002). Probabilistic failure analysis of nuclear piping with empirical study of Taiwan's BWR plants, International Journal of Pressure Vessels and Piping, 79(7), pp. 483–92. Doi: 10.1016/S0308-0161(02)00061-3

[10.] Rudland D., Wolterman, R. and Wilkowski, G. (2003). Impact of PWSCC and Current Leak

Detection on Leak-Before-Break, Emc2 final report to NRC, January 31.

[11.] Meireles, M.R.G., Almeida, P.E.M., Simoes, M.G. (2003). A comprehensive review for industrial applicability of artificial neural networks, IEEE Trans. Ind. Electron, Vol. 50, n. 3, pp.585–601. Doi: 10.1109/TIE.2003.812470

[12.] Mannan, S.L., Chetal, S.C., Baldev Raj and Bhoje, S.B. (2003). Proceedings of the seminar on Materials R & D for PFBR, Eds. S. L. Mannan and M. D. Mathew, IGCAR, Kalpakkam.

[13.] JONES, R. (2004). Mitigation corrosion problems in LWRs via chemistry changes, Water Chemistry of Nuclear Reactor Systems (Proc. Int. Conf. San Francisco, 2004), EPRI report 1011579, Palo Alto, CA.

[14.] INTERNATIONAL ATOMIC ENERGY AGENCY. (2005). Assessment and Management of Ageing of Major Nuclear Power Plant Components Important to Safety: BWR Pressure Vessels, IAEA-TECDOC-1470, IAEA, Vienna.

[15.] Guedri, A., Tlili, S., Merzoug, B., Zeghloul, A. (2007). An artificial neural network model for predicting mechanical properties of CMn (V-Nb-Ti) pipeline steel in industrial production conditions, International Review of Mechanical Engineering, vol. 1, n. 5 pp. 397-405.

[16.] Zuo, M.J., Tian, Z., Huang, HZ. (2007). Neural Networks for Reliability-Based Optimal Design. In: Levitin, G. (eds) Computational Intelligence in Reliability Engineering. Studies in Computational Intelligence, vol 40. Springer, Berlin, Heidelberg. https://doi.org/10.1007/978-3-540-37372-8_7

[17.] Cardoso, J.B., de Almeida, J.R., Dias, J.M., Coelho, P.G. (2008). Structural reliability analysis using Monte Carlo simulation and neural networks, Advances in Engineering Software, 39(6), pp. 505–13. Doi: 10.1016/j.advengsoft.2007.03.015

[18.] Garcia, C., de Tiedra, M.P., Blanco, Y., Martin, O., Martin, F. (2008). Intergranular corrosion of welded joints of austenitic stainless steels studied by using an electrochemical minicell, Corros. Sci., 50(8), pp. 2390–2397. DOI:10.1016/j.corsci.2008.06.016

[19.] Lo, K.H., Shek, C.H., Lai, J.K.L. (2009). Recent developments in stainless steels, Mater. Sci. Eng. R Reports, pp. 39–104. DOI: 10.1016/j.mser.2009.03.001

[20.] Guedri, A., Zeghloul, A., Merzoug, B. (2009). Reliability analysis of BWR piping including the effect of residual stresses, International Review of Mechanical Engineering, 3(5), pp. 640–5.

[21.] Khaleel, M., Simonen, F. (2009). Evaluations of Structural Failure Probabilities and Candidate Inservice Inspection Programs, NUREG/CR-6986; PNNL-13810, Pacific Northwest National Laboratory, Richland, WA.

[22.] Guedri, A., Djebbar, Y., Khaleel, M., Zeghloul, A. (2012). Structural Reliability Improvement Using In-Service Inspection for Intergranular Stress Corrosion of Large Stainless Steel Piping, In Applied Fracture Mechanics, Alexander Belov (Ed.), pp.331-358.

[23.] Guedri, A. (2013). Effects of remedial actions on small piping reliability, Proceedings of the Institution of Mechanical Engineers, Part O: Journal of Risk and Reliability, 227(2), pp. 144–61. Doi: 10.1177/1748006X13477798

[24.] Guedri, A. (2013). Reliability analysis of stainless-steel piping using a single stress corrosion cracking damage parameter, Int. J. Press. Vessel. Pip, vol. 111–112, pp. 1–11. Doi: 10.1016/S0308-0161(02)00061-3

[25.] Cheng, C.Q., Klinkenberg, L.I., Ise, Y., Zhao, J., Tada, E., Nishikata, A. (2017). Pitting corrosion of sensitised type 304 stainless steel underwet–dry cycling condition, Corros. Sci., 118, pp. 217–226, DOI: 10.1016/j.corsci.2017.02.010.

[26.] Kim, S.H., Goni, M.N., Chang, YS. (2018). Probabilistic Assessment of Nuclear Piping Integrity by Considering Environmental Fatigue and Stress Corrosion Cracking. In: Ambriz, R., Jaramillo, D., Plascencia, G., Nait Abdelaziz, M. (eds) Proceedings of the 17th International Conference on New Trends in Fatigue and Fracture. NT2F 2017. Springer, Cham. https://doi.org/10.1007/978-3-319-70365-7_16

[27.] Boutelidja, R., Guedri, A., Belyamna, M.A., Merzoug, B. (2019). Environmental effects on the reliability of an AISI 304 structure, Frat.ed Integrita Strutt, vol. 13, n. 50, pp. 98–111. Doi: 10.3221/IGF-ESIS.50.10

[28.] Wen, K., He, L., Liu, J., Gong, J. (2019). An optimization of artificial neural network modeling methodology for the reliability assessment of corroding natural gas pipelines, Journal of Loss Prevention in the Process Industries, 60(March), pp. 1–8. Doi: 10.1016/j.jlp.2019.03.010

[29.] Tokuda, S., Muto, I., Sugawara, Y., Hara, N. (2020). Pit initiation

on sensitized Type 304 stainless steel under applied stress": Correlation of stress, Cr-depletion, and inclusion dissolution, Corros. Sci., 167, p. 108506. DOI: 10.1016/j.corsci.2020.108506

[30.] Solanki, R.B., Kulkarni, H.D., Singh, S., Varde, P. V., Verma, A.K. (2020). Reliability assessment of passive systems using artificial neural network based response surface methodology, Annals of Nuclear Energy, 144. Doi: 10.1016/j.anucene.2020.107487

[31.] Pourahmadi, M., Saybani, M. (2022). Reliability analysis with corrosion defects in submarine pipeline case study, Oil pipeline in Ab-khark island, Ocean Engineering, Vol. 249. Doi:10.1016/j.oceaneng.2022.110885

[32.] Zhang, H., Tian, Z. (2022). Failure analysis of corroded high-strength pipeline subject to hydrogen damage based on FEM and GA-BP neural network, International Journal of Hydrogen Energy, 47(7), pp. 4741–58. Doi: 10.1016/j.ijhydene.2021.11.082

[33.] Belyamna, M.A., Zeghida, C., Tlili, S., Guedri, A. (2022). Piping reliability prediction using Monte Carlo simulation and artificial neural network, Procedia Structural Integrity, Vol. 41, pp.372-383. https://doi.org/10.1016/j.prostr.2022.05.043